Project Report on

Stochastic Resonance in the Lorenz Model: Numerical and Theoretical Investigations

By

Vishal Singh

Indian Institute of Science Education and Research, Kolkata

Under the supervision of

Dr. Pankaj Kumar Mishra

At

Indian Institute of Technology, Guwahati

Contents

1 Introduction

The Lorenz system of equations is one of the most studied models in nonlinear dynamics, owing to the wide range of fascinating and often counter intuitive results that the seemingly simple system displays. A number of real world phenomena, such as weather predictions and biological systems, have been modeled based on these equations. Since fluctuation phenomena are typical for all real systems due to the discrete structure of matter and cannot be eliminated in principal, the behaviour of any dynamical system in presence of external perturbation has always been an important field of study. The presence of noise in any dynamical system was so far believed to boost the degree of disorder in the system. Contrary to that belief, studies have shown that in nonlinear systems noise can induce *stochastic resonance* (SR). This leads to the formation of more regular structures. This is manifested by increase in the degree of coherence, amplification of weak signals and growth of the signal-to-noise ratio. In other words, noise can play a constructive role, enhancing the degree of order in a system.

The term stochastic resonance was originally used in the context of a bistable oscillator model that was proposed to describe the switching of earth's climate between ice ages and periods of relative warmth. In 1981, Benzi *et al.* used the Langevin equation to show that a dynamical system subject to both periodic forcing and random perturbation may show a resonance behaviour which is absent when either the forcing or the perturbation is absent. They found that an analytical theory of SR cannot be developed for Lorenz model but we can discuss it qualitatively.

Around a decade later, Anishchenko *et al.* used high intensity noise on low frequency carrier signals to study the effects of SR through frequency and amplitude modulation. They showed that distortions of the signal can be minimized by choosing optimal noise and tuning operating characteristics of the system. Quantitatively, they used a maximum value of coherence function to indicate the presence of SR.

In 1994, Gao *et al.* studied the Lorenz equations in the parameter range in and slightly above the metastable chaos regime with periodic forcing. They observed that noise induces oscillatory motions with well-defined periods, a phenomenon similar to stochastic resonance. However, without a weak periodic forcing, noise annihilates the two stable fixed point solutions, leaving the originally transient metastable chaos the only observable. They also found that noise may induce hopping between one of the fixed point solutions and the metastable chaos, thereby leading to a three-state intermittency.

In this report, the Lorenz system under various parameter conditions is studied. In particular, the evolution of the dynamic variables with time and their trajectories on the phase plane are discussed. This is followed by the study of the system in the presence of an external Gaussian noise. In the next section, an analytical method to distinguish noise-induced chaos from deterministic chaos is applied. The report is concluded by introducing a weak periodic forcing in the system and the presence of stochastic resonance is checked by varying the noise intensity.

2 The Lorenz Equations

In 1963, Edward Lorenz, a meteorologist at the Massachusetts Institute of Technology, was trying to construct mathematical models for weather and climate. He came up with a set of three non-linear ordinary differential equations to mathematically describe an oversimplified model of convection rolls in the atmosphere. The Lorenz equations are given by:

$$\dot{x} = \sigma(y - x) \tag{1}$$

$$\dot{y} = rx - y - xz \tag{2}$$

$$\dot{z} = xy - \beta z \tag{3}$$

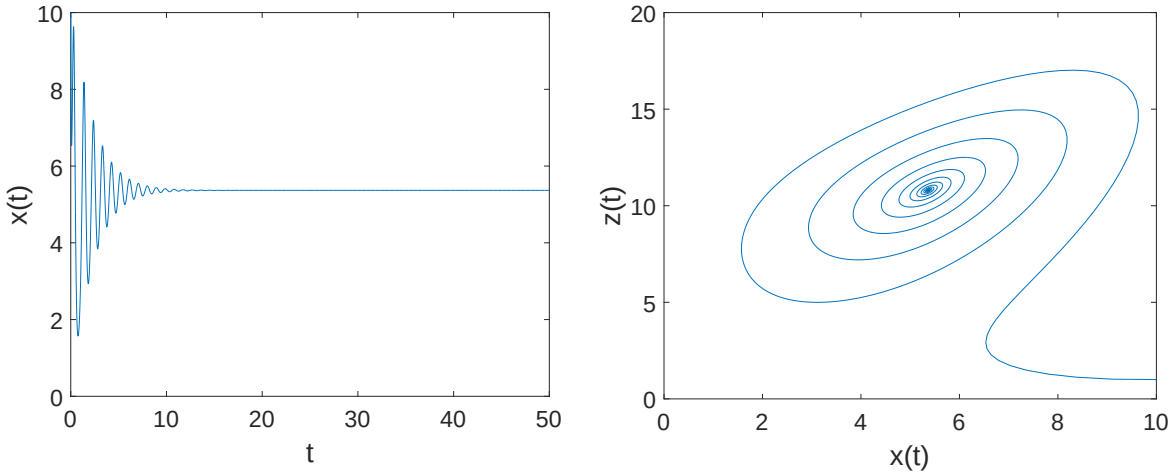

Figure 1: Time series of $x(t)$ and phase space plot for $r = 11.8$. The initial conditions used are $(10, 0, 1)$.

where σ is the Prandtl number, r is the Rayleigh number in a fluid convection model and β is related to the aspect ratio of the rolls in the convection problem. The usual values of parameters used are $\sigma = 10$ and $\beta = \frac{8}{3}$. In case of the convection model, x is proportional to the intensity of convective motion, y is proportional to the temperature difference between ascending and descending currents. Similar signs of x and y denote that warm fluid is rising and cold fluid is descending. The variable z is proportional to the distortion of the vertical temperature profile. A positive value of z indicates that the strongest gradients occur near the boundaries.

Dynamics of the Lorenz System

The Lorenz system of equations leads to different kinds of trajectories depending on the values of the parameters as well as the initial conditions. The Lorenz system is a dissipative system, which means that the phase space volume always contracts with flow.

The Lorenz system has three fixed points, which are given by: $C_0 = (0, 0, 0)$ and $C_\pm = (\pm\sqrt{\beta(r-1)}, \pm\sqrt{\beta(r-1)}, r-1)$. For $r < 1$, C_0 is a stable fixed point and C_+ and C_- do not exist, i.e, all trajectories lead to the origin. For $r > 1$, C_0becomes unstable and the system ends up in either of the two fixed points, C_+ or C_-, depending on the initial conditions. For $r < 13.926$, the trajectories are similar to that of a damped periodic oscillator. They start at the initial conditions, oscillate periodically and gradually reaches one of the steady state points, C_+or C_-. In Fig.1, we have shown the time evolution for the x co-ordinate of the Lorenz equations, and the phase space plot of $x(t)$ vs $z(t)$. We see that $x(t)$ displays an oscillatory motion which gradually damps and reaches a constant value 5.367. On examining the temporal evolution of the other two co-ordinates, we find that the system settles at $(5.367, 5.367, 10.8)$, i.e, the fixed point C_+. The phase space plot also shows the presence of a fixed point attractor at C_+.

For $r \in (13.926, 24.06)$, the system exhibits *metastable chaos*. This means that for certain initial conditions, the system exhibits chaos for an extensive period of time, before settling into either of the two fixed points $C_\pm$. This behaviour is generally encountered for values of r close to 24.06. Fig.2 shows the time series for $x(t)$ and phase space plot $x(t)$ vs $z(t)$ for $r = 22.3$. We see that the system behaves chaotically and shows aperiodic irregular oscillations about the two fixed points for some time, and then becomes oscillatory about one of the steady states, and finally tends to the steady state solution.

When $r \in (24.06, 24.72)$, the system has two stable fixed points, C_+ and C_-, and a *strange attractor*. Depending on the initial conditions, the system settles in either of these three attractors.

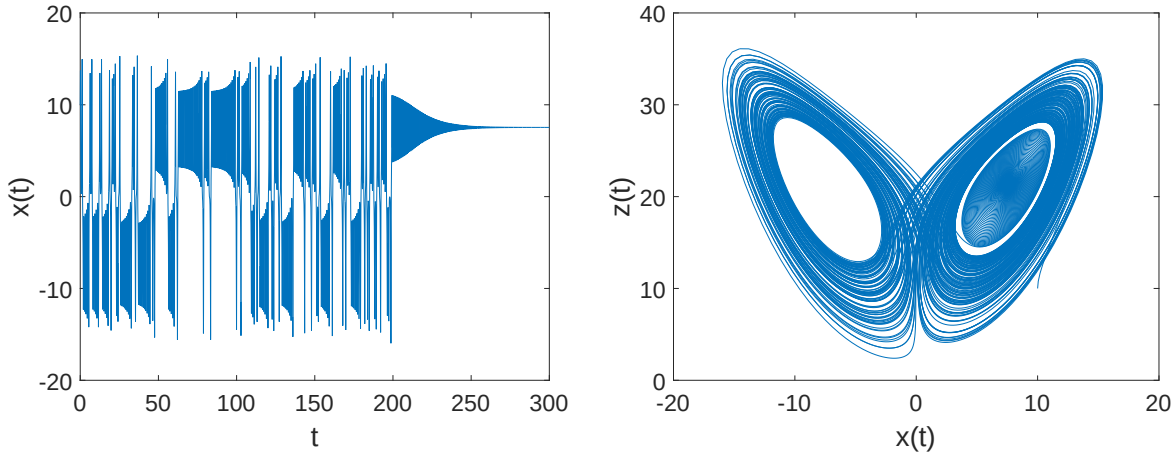

Figure 2: Time series of $x(t)$ and phase space plot for $r = 22.3$. The initial conditions used are $(10, 10, 10)$.

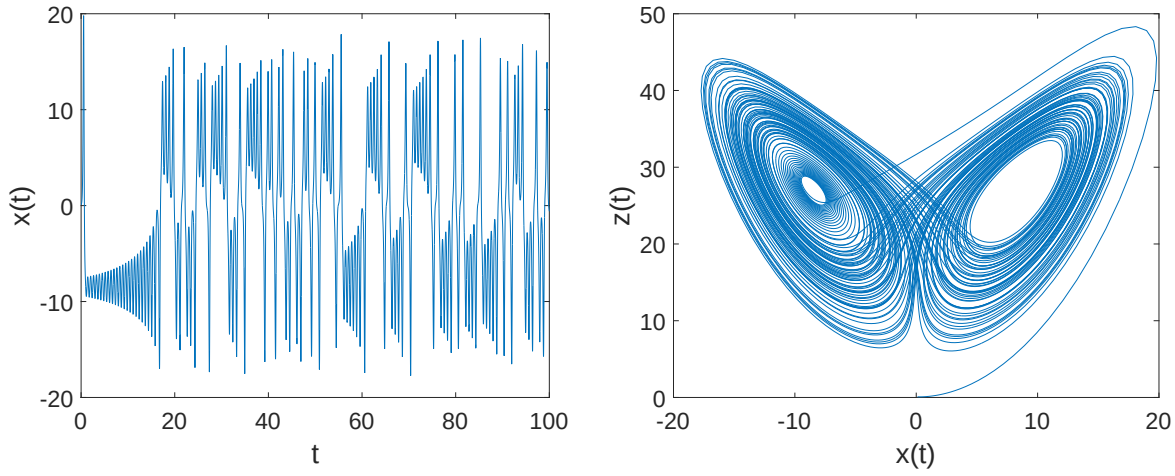

Figure 3: Time series of $x(t)$ and phase space plot for $r = 28$.

As r is increased beyond r_H, where $r_H = \frac{\sigma(3+\beta+\sigma)}{\sigma-\beta-1}$, the system undergoes a transition to chaos. This transition to the chaotic state occurs at $r = r_H$ through Hopf bifurcation. The stable steady state solutions vanishes, and the system behaves like a strange attractor. The attractor is stable in the sense that almost all initial conditions get pulled into the attractor and traces the same butterfly-shaped trajectory in phase space. A small change in initial conditions, or a small perturbation, does not alter the overall shape of the attractor. However, the temporal evolution of individual trajectories are unstable. They show *sensitive dependence on initial conditions*, which means that two orbits starting extremely close to each other diverges exponentially. This exponential divergence is characterised by a large positive value of the *Lyapunov exponent*. Hence, although it is certain that the orbits will always follow a bounded trajectory on the attractor, the exact paths of the orbits are unpredictable. This unpredictability in a deterministic system, i.e., in the absence of any stochastic component, is a result of the non-linearity. Fig.3 shows the classic model of the Lorenz attractor with $\sigma = 10, \beta = \frac{8}{3}$,$r = 28$ and initial conditions $(0.1, 0.1, 0.1)$.

3 Effect of Noise on the Lorenz system

In this section, we study the effect of a stochasticity on the Lorenz equations. For this purpose, we study the Lorenz system in details for two different values of the Rayleigh number : $r = 24.01$ and $r = 30.0$. We know that in the absence of noise, the Lorenz system evolves periodically to a stable fixed point for $r = 24.01$, as shown in Fig.4(a). For $r = 30.0$, the clean Lorenz system exhibits chaos, as shown in Fig.4(b). We have used the Runge-Kutta 4th order method to numerically solve the Lorenz equations (1)-(3) with initial conditions $x_0 = 0.1, y_0 = 0.1, z_0 = 0.1$ and time step of $h = 0.01$.

Now, a Gaussian white noise is introduced in the y equation (2).

$$\dot{y} = rx - y - xz + D\xi(t) \tag{4}$$

where $r = 24.01$ and $D\xi(t)$ is white Gaussian noise with $\langle \xi(t) = 0 \rangle$ and $\langle \xi(t)\xi(t') = \delta(t - t') \rangle$ and variance D^2. Physically, this noise accounts for fluctuations in the temperature difference between the ascending and descending currents in the fluid convection model. We observe that the addition of noise results in the transition of the trajectory from the steady state to the chaotic state, shown in Fig.5.

The transition of the system from periodic to chaotic regime can also be noted distinctly from the *power spectral density* (PSD) plot of the signal. The PSD of a signal gives the power present in the signal per unit frequency as a function of frequency. The PSD of signal $x(t)$ as a function of frequency ω is defined as

$$PSD_x(\omega) = \frac{(\Delta t)^2}{T} \left| \sum_{k=1}^{N} x_k e^{-2\pi i \omega k} \right|^2 \tag{5}$$

where x_k is the discrete value of the variable at time $t_k = k\Delta t$, with Δt as the sampling time, ω is the frequency of the fluctuation and T is the total time interval for which data is considered. We have generated the PSD using the Fast Fourier Transform (FFT) algorithm, with sampling time $\Delta t = 0.01$. A sharp peak in the PSD at a given frequency and its harmonics implies that the signal is periodic and has the frequency corresponding to the peak. Fig.6 shows the power spectral density of the signal $x(t)$ plotted against frequency. We see that in the absence of noise or for smaller values of noise, a distinct peak in the spectral density is observed, along with harmonic peaks. This indicates that the system is periodic. As noise is increased, the peaks start disappearing and at $D = 0.05$, the peaks vanish completely indicating that the system becomes completely chaotic.

We further plot the curve of $logA$ vs $log(D^2)$, where A is the average amplitude of oscillation of $x(t)$ and D represents the noise strength. This is shown in Fig.7. The slope is found to be 0.50. This square root dependence of the amplitude and the noise level is a characteristic of Hopf bifurcation. As stated earlier, the transition of the system from periodic to chaotic due to increasing r, i.e, in the absence of noise, also occurs through Hopf bifurcation. Further, for $r = 24.01$, the system shows a time series

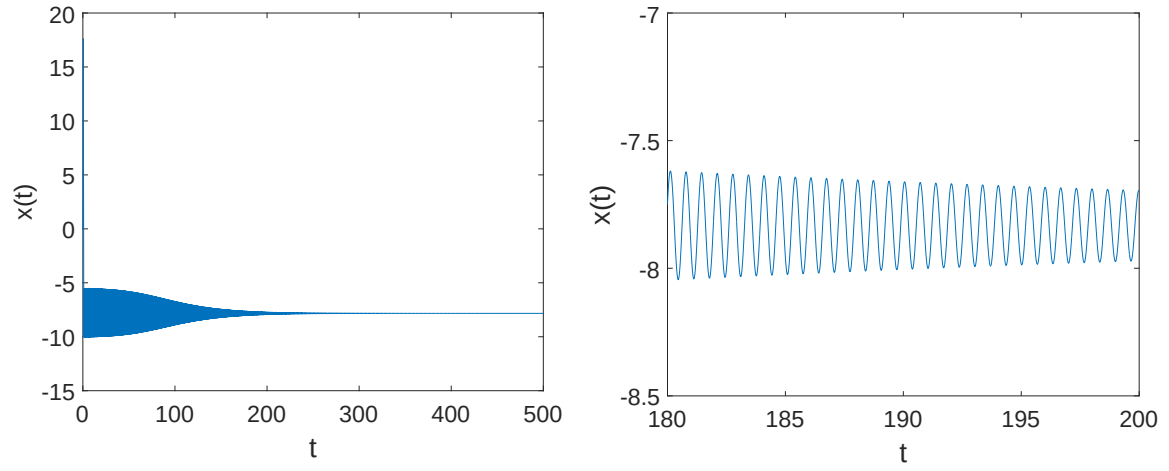

(a)

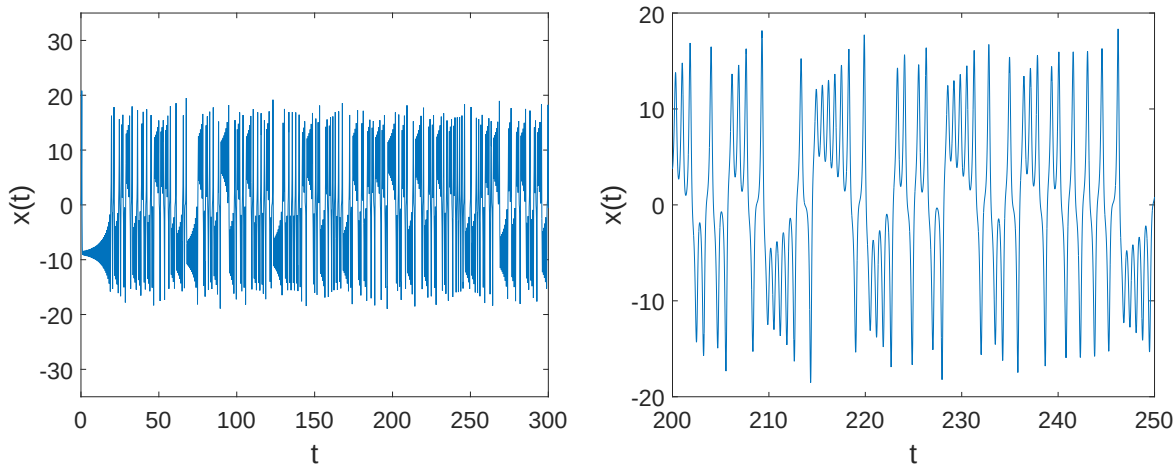

(b)

Figure 4: Time series of $x(t)$ for $(a) r = 24.01$ and $(b) r = 30.0$. The temporal evolution for a narrower time range has been shown for both the cases in the right hand side figures to provide a clear visualisation of the periodic nature of $x(t)$ for $r = 24.01$, and the chaotic oscillations of $x(t)$ for $r = 30.0$.

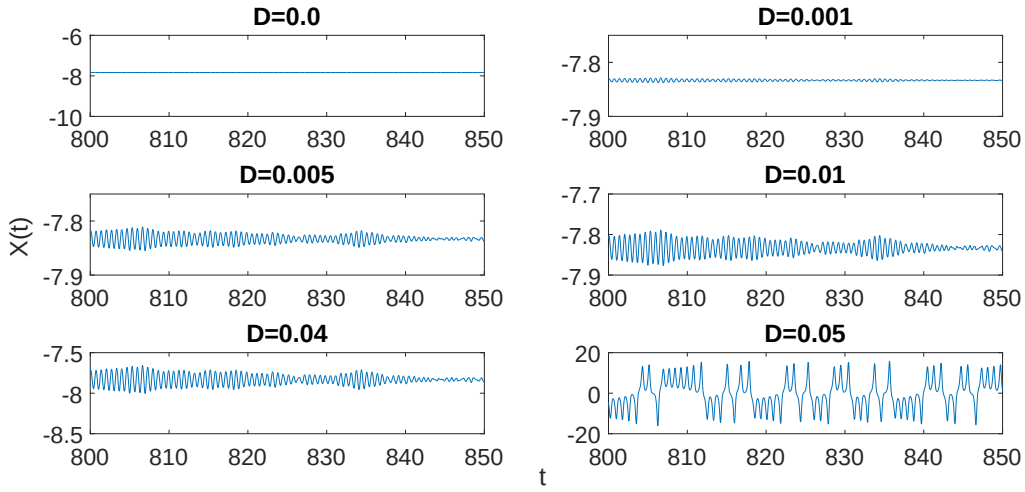

Figure 5: Time series $x(t)$ for $r = 24.01$ with different values of noise D. We have shown the plots for a range of $t = 800$ to $t = 850$ to see the gradual transition to chaos with greater clarity.

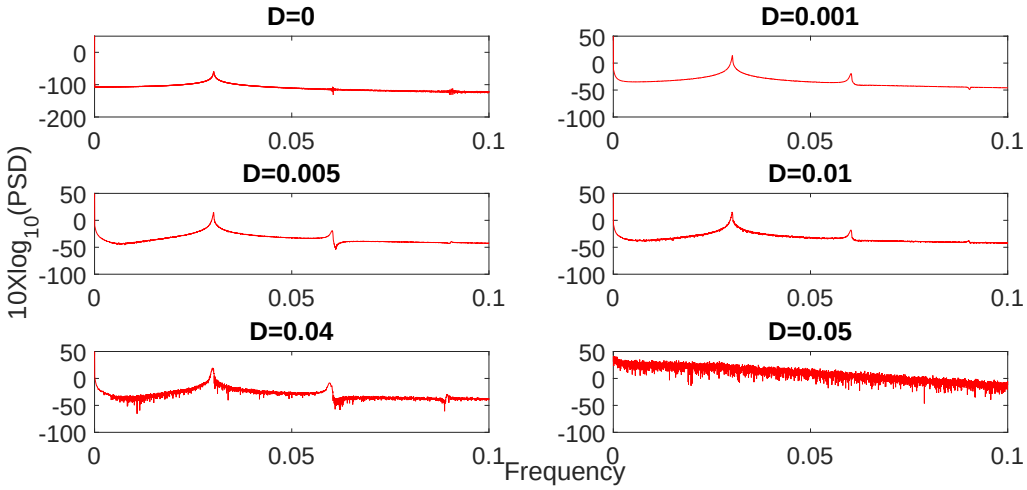

Figure 6: Power spectral density plot of $x(t)$ at $r = 24.01$ for varying noise strength.

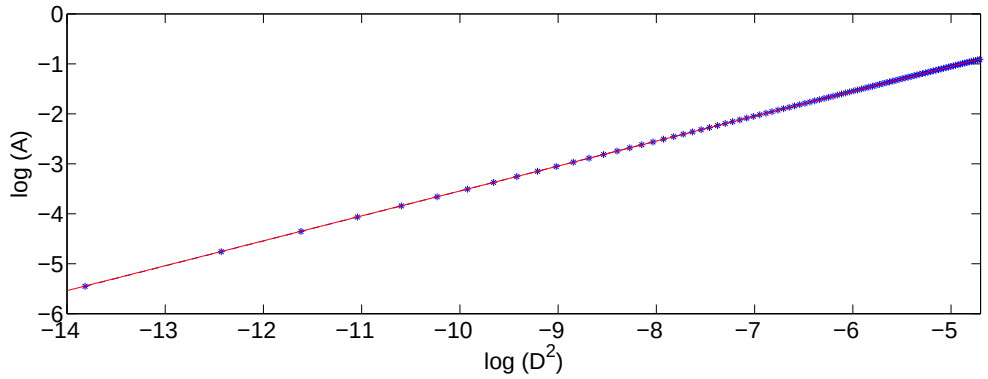

Figure 7: $log - log$ amplitude A of $x(t)$ versus noise strength D^2 for $r = 24.01$ and $D = 0.05$.

similar to that of the clean Lorenz system for $r = 30.0$. In other words, the introduction of noise to the system is equivalent to increasing the value of r. In the following section, we compare the noise-induced chaos at $r = 24.01$ to deterministic chaos at $r = 30$ and see whether they are characteristically similar.

4 Characterisation of chaos

In this section, we check whether the chaos induced by noise for smaller values of r is characteristically similar to the chaos produced in the system due to higher values of r in the absence of noise. For this purpose, we use the dynamical test for deterministic chaos. We use the time delay embedding procedure to construct vectors of the form $X_n = [x_l, x_{l+L}, ..., x_{l+(d-1)L}]$ where L is the delay time and d is the embedding dimension. We chose d and L such that the optimization criterion as specified by Gao *et al.* is satisfied. We compute a series of $\zeta(n)$ curves defined by

$$\zeta(n) = \left\langle ln\left(\frac{||X_{l+n} - X_{m+n}||}{X_l - X_m}\right)\right\rangle \tag{6}$$

with $s \leq ||Xl - Xm|| \leq s + \Delta s$, where geometrically, $(s, s + \Delta s)$ represents a shell. The angular brackets denote ensemble average over all possible pairs of (X_l, X_m).

The computations are carried out for a series of shells of arbitrary radii. The integer n corresponds to the evolution time. In absence of noise, the chaotic behaviour is inherent to the system. In this case, for small values of n, $\zeta(n)$ is independent of the radius of the shells used, and is linearly increasing. Hence the linear region of $\zeta(n)$ forms a distinct envelope for a sequence of shells, whose slope corresponds to a large positive Lyapunov exponent. The fact that the Lyapunov exponent is independent of the shells used for computation characterizes the system as truly chaotic. However, in case of stochastic process, $\zeta(n)$ depends on the radius of the shell used. Hence, as noise is added, the envelope is destroyed. The slope of the graph then changes depending on the shell considered, and implies that the process becomes stochastic. This distinguishes true chaos from noise-induced chaos. In Fig., we have plotted the variation of $\zeta(n)$ with the evolution parameter n for 3 different cases. We have used 3 different shells, given by $(0.1n, 0.5n)$, where $l = 4, 5, 6$. We observe a linear increase in $\zeta(n)$ for smaller values of n. In Fig.8(c), where noise is absent, the linear region of $\zeta(n)$ forms a common envelope for the 3 different shells. We observe that with a decrease in r and increase in the noise D, the envelope breaks. This helps us distinguish between inherent chaos in the system and noise-induced stochastic process. The slope of the linear envelope in Fig.8(c), which serves as an estimate of the largest Lyapunov exponent, is found to be 0.1094.

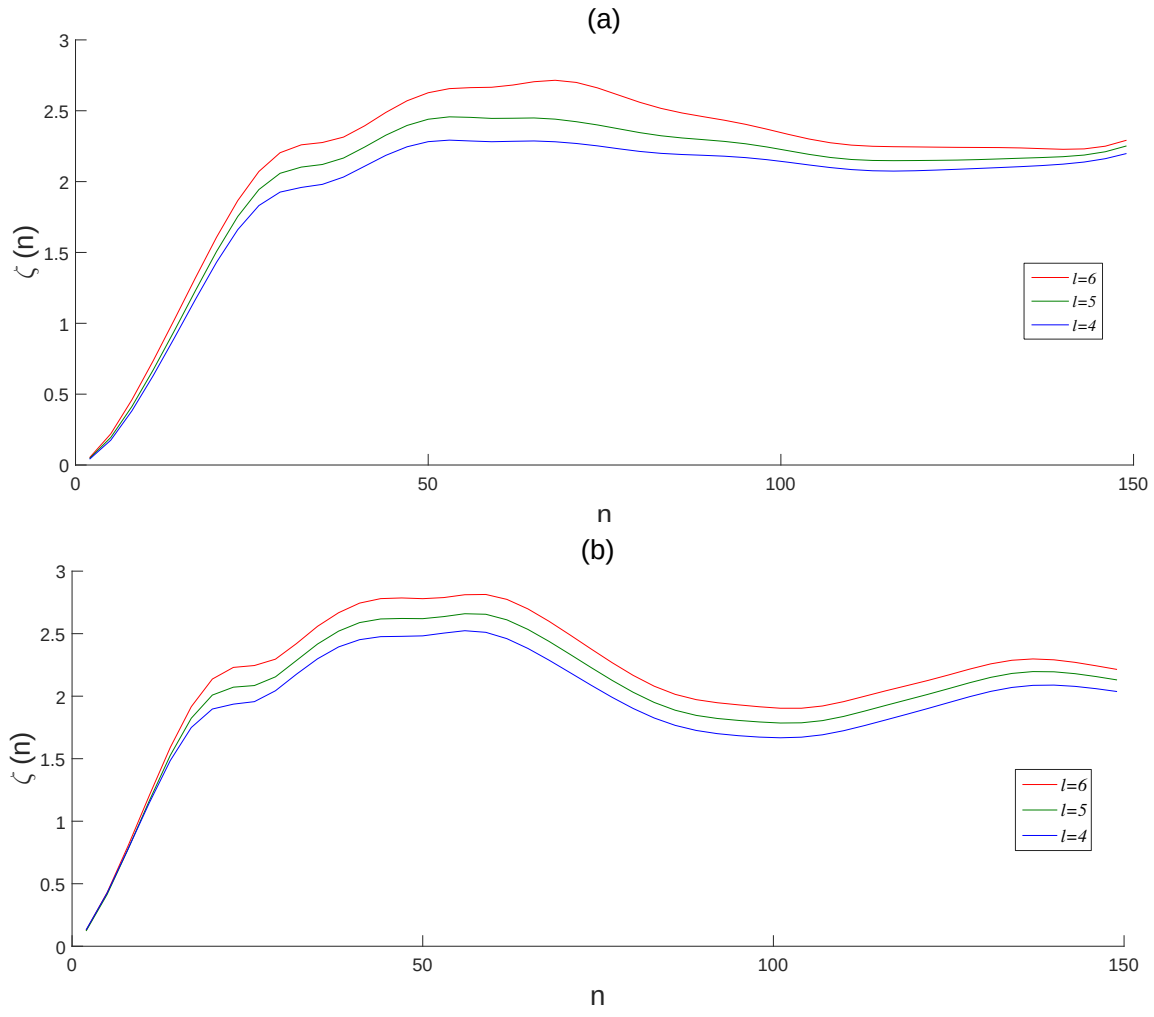

Figure 8: Plots showing variation of $\zeta(n)$ with n for $(a) r = 24.01, D = 0.05, (b) r = 30.0, D = 0.0$. The delay vector was constructed with embedding dimension $d = 10$ and delay time $L = 3$.

5 Stochastic resonance in Lorenz System

In this section, we observe the behaviour of the Lorenz system under a periodic force of small amplitude. Our aim is to study the combined effect of noise and periodic force on the system, and check whether the system shows stochastic resonance for optimal characteristics of the noise. In their review of stochastic resonance, Anishchenko *et al* states that SR can be observed only in those non-linear systems for which a characteristic time scale dependent on the noise intensity is available. For the case of Lorenz model, this characteristic time scale is usually defined by the *mean residence time* of the system. The residence time of a bistable system is defined as the average time the system spends in each state before switching to the other state. In the chaotic regime, the Lorenz system displays a similar switching behaviour between the two lobes of the strange attractor. The residence time is calculated as the average time the system spends in one lobe of the Lorenz attractor before switching to the other lobe.

To study the phenomenon of SR in the Lorenz system, we choose r =24.01. We drive the system from periodic to chaotic by adding an external noise of varying intensity, and study the characteristics of the system. We begin by adding a periodic force of small amplitude to equation (4) :

$$\dot{y} = rx - y - xz + D\xi(t) + Acos(\omega_0 t) \tag{7}$$

where $Acos(\omega_0 t)$ is a periodic force of amplitude A and frequency ω_0. The frequency of the periodic force is taken to be $2\pi/\tau$, where τ is the *mean residence time* of the system in absence of external noise. In Fig.9 we have shown the time series and PSD of $x(t)$ for $r = 24.01$ and $D = 0.05$ with different amplitudes of the periodic force. It is clear from both set of plots that as the amplitude of the perodic force is increased, the trajectory of the Lorenz system transitions from chaotic to more and more periodic. In the latter case, This is because beyond a certain amplitude of the force, the amplitude of the perturbation is of so large that the system is forced to follow the driving frequency of the periodic forcing. Thus, to guarantee that the response behavior is due to "resonance" and not due to "forcing", it is important to keep the amplitude of the periodic force sufficiently low. From the plots, we see that choosing the periodic force amplitude to be $A = 0.1$ does not result in force-driven periodicity. Hence we set the amplitude as $A = 0.1$.

SR in a system can be proven using a number of results, such as minimum entropy to indicate enhanced order in the system, or a sharp peak in the signal-to-noise ratio (SNR) of the system for a certain noise intensity. In this report, the later method is used. SNR compares the level of a desired signal to the level of background noise. SNR is defined as the ratio of signal power to the noise power, often expressed in decibels. Mathematically, it can be defined as

$$SNR = 2 \sum_{\omega_0 - \Delta\omega}^{\omega_0 + \Delta\omega} S(\omega)\delta\omega / S_N(\omega_0) \tag{8}$$

where ω_0 is the frequency of the periodic force and $S_N(\omega_0)$ is the value of the power spectral density corresponding to frequency ω_0. SNR is calculated as the area under the peak in the PSD plot at $\omega = \omega_0$. For a system subjected to a weak signal and noise, the SNR increases with the noise intensity, reaches a maximum value for a certain intensity of noise, and then gradually decreases. This shows that there is an optimal noise level at which the periodic component of the signal is maximized. This is a conclusive proof of SR in the system.

Fig.10 shows that the SNR vs noise intensity plot attains a maximum at $D = 0.3$. This peak in the SNR vs D plot implies the presence of stochastic resonance in the system for $D = 0.3$. The corresponding time series plot and PSD plot are shown in Fig 11. We see that the PSD of the dynamic variable $x(t)$ has a spike at the frequency at which the PSD of the periodic signal shows a peak. This implies that for $D = 0.3$, the Lorenz system has a periodic element characterised by the frequency of the driving force. This is the characteristic of SR in the system.

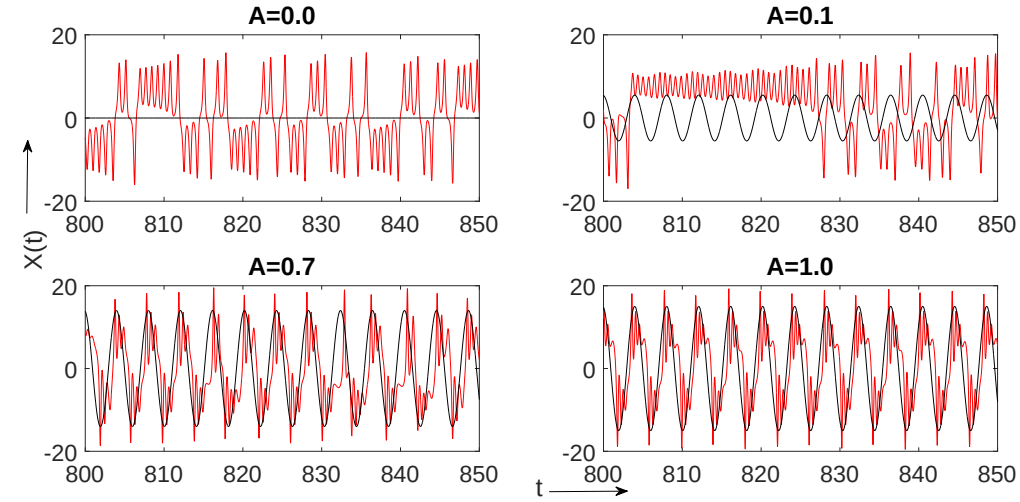

(a)

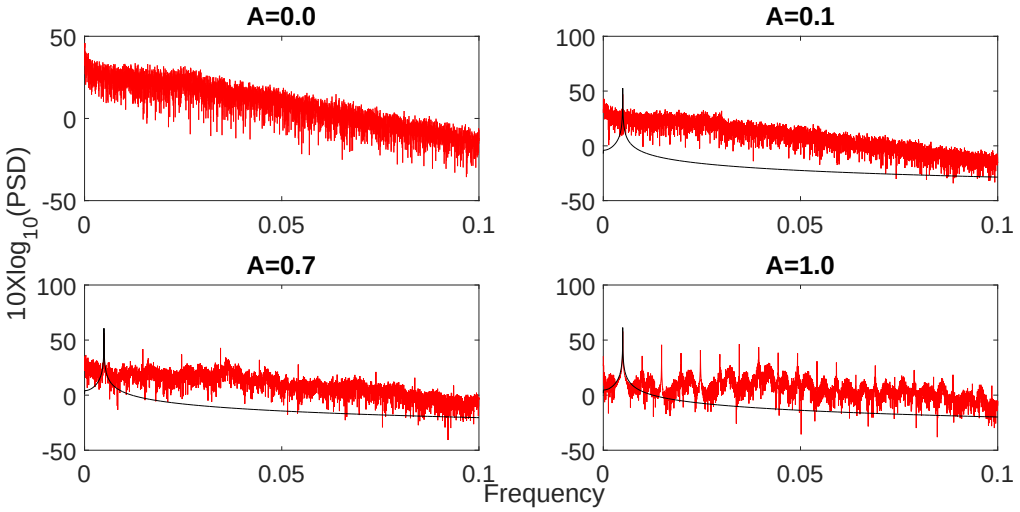

(b)

Figure 9: (a) Temporal evolution of $x(t)$ for $r = 24.01$ and $D = 0.05$ with varying amplitude of periodic force. The black curves represent the external periodic force scaled up to $20X$. (b) PSD of $x(t)$ for $r = 24.01$ and $D = 0.05$ with varying amplitude of periodic force. The black curves show the PSD plots of the external periodic force.

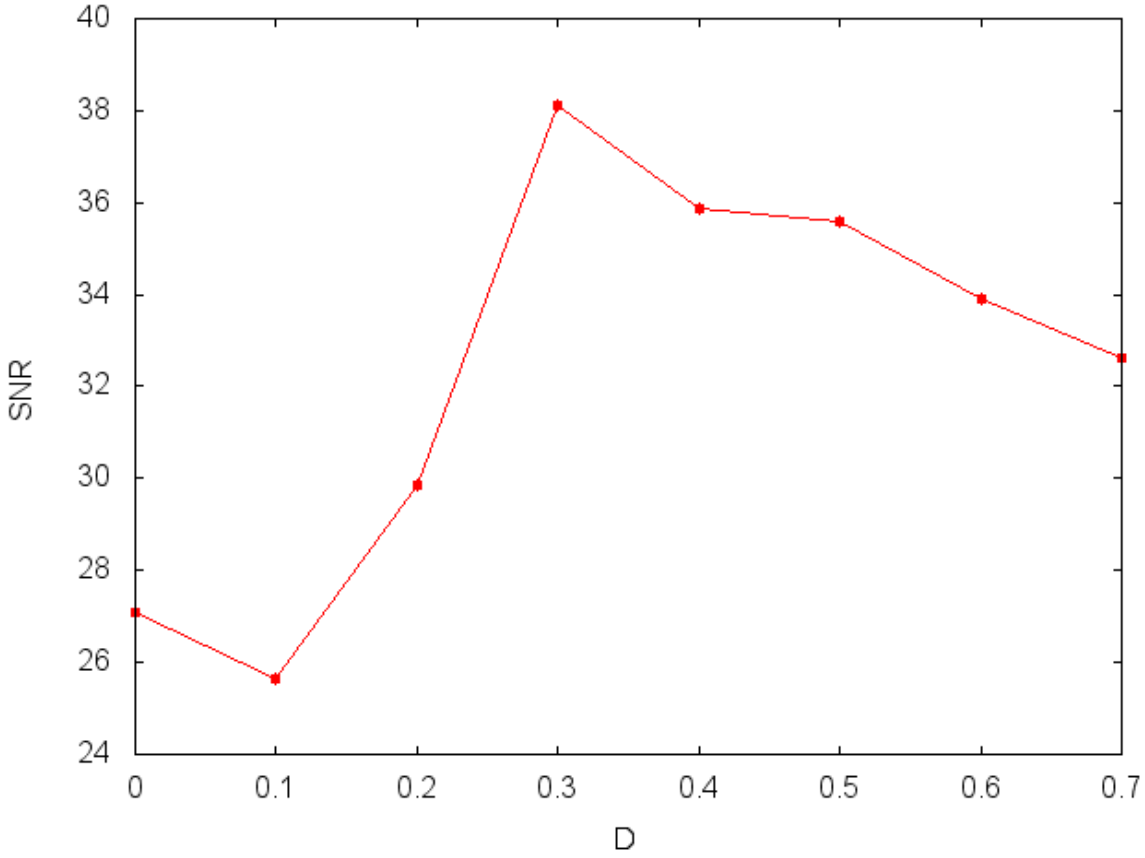

Figure 10: Signal to noise ratio vs noise intensity$D$ for $r = 24.01, A = 0.1$. The SNR reaches a maximum at $D = 0.3$ and exhibits SR.

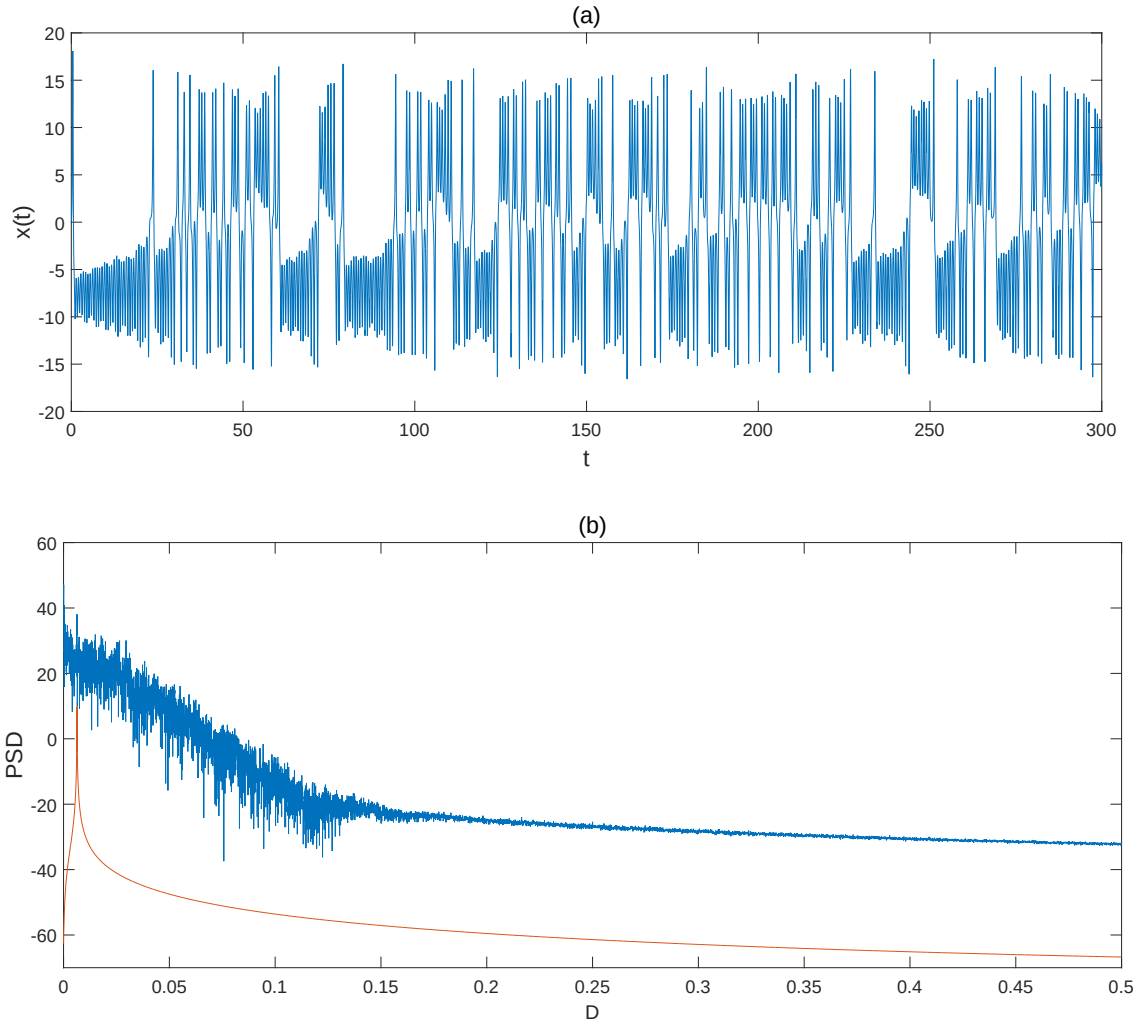

Figure 11: (a) Time series of $x(t)$ for $r = 24.01, D = 0.3$. (b) PSD vs D plot for $x(t)$ and periodic force.

6 Conclusion

In this report, we presented a brief analysis of the Lorenz system of equations and how the system responds to external perturbation. In the first section, we studied the general dynamics of the system in absence of noise. We observed that the system displays characteristically different behaviour for different values of parameters. We studied the temporal evolution of the dynamic variables and their phase space trajectories as the system undergoes transition from periodic to metastable to chaotic nature with varying r. We saw that the system undergoes transition to chaotic state for a particular value of r which is independent of the initial conditions, and this transition occurs through Hopf bifurcation. In the next section, we introduced an external white Gaussian noise in the system and studied the aforementioned characteristics. It was seen that an external noise beyond a certain threshold value (depending on the value of r) drives the system from periodic to chaotic. This transition also occurs through Hopf bifurcation. Thus it can be concluded that the effect of adding an external noise to the system at low values of r is essentially similar to increasing the value of r in absence of noise. In the next section we used a pre-established analytical method to compare the inherent chaotic nature of the system to the noise-induced chaotic behaviour. In the concluding section, we introduced a weak periodic forcing to the system in the presence of noise and observed that for an optimal noise intensity, the signal to noise ratio attains a maximum. We concluded that the Lorenz system exhibits stochastic resonance in the presence of an external periodic driving force and noise.

References

[1] R. Benzi, A. Sutera, and A. Vulpiani, J. Phys. A: Mathematical and General, **14**(11), (1981).

[2] B. McNamara and Kurt Wiesenfeld. Theory of stochastic resonance. Phys. Rev. A, **39**:4854–4869, (1989).

[3] V. S. Anishchenko, A. B. Neiman, F. Moss, and L. Schimansky-Geier, Rev. Top. Prob., **42**(1):7–36, (1999).

[4] E. N. Lorenz. Deterministic nonperiodic flow. J. Atmos. Sci.,**20**(2):130–141,(1963).

[5] J. B. Gao, Wen-wen Tung, and N. Rao, Phys. Rev. Lett. **89**, 254101 (2002).

[6] S.H. Strogatz. Nonlinear Dynamics And Chaos. Studies in nonlinearity. Sarat Book House, 2007.

[7] Jing Hu and Jianbo Gao, Vincent A. Billock, Wen-Wen Tung, Int. J. Bifur. and Chaos **18**, No. 6 1749–1758, (2008).

[8] A. Zippelius, M. Lucke, J. Stat. Phys., **24**(2), (1981).

[9] R. Benzi, J-F Pinton, arXiv:1104.4417 [nlin.CD], (2011).

[10] J. B. Gao and Z. Zheng, Phys. Rev. E, **49**, No.5, (1994).

[11] L.Alfonsi, L.Gammaitoni, S.Santucci, and A.R.Bulsara, Phys. Rev. E, **62**(1):299-302, (2000)

[12] Sinha:1999)S.Sinha, Physica A 270: 204-214, (1999)